ELSEVIER

Surface Science 470 (2000) 141–148

SURFACE SCIENCE

www.elsevier.nl/locate/susc

Diffraction of correlated electron pairs from crystal surfaces

S. Samarin [a,*], J. Berakdar [a], O. Artamonov [b], H. Schwabe [a], J. Kirschner [a]

[a] *Max-Planck-Institut für Mikrostrukturphysik, Weinberg 2, D-06120 Halle, Germany*

[b] *Research Institute of Physics, St. Petersburg University, Uljanovskaja 1, Petrodvoretz, 198904 St. Petersburg, Russian Federation*

Received 2 June 2000; accepted for publication 25 August 2000

Abstract

The spectra of the internal energy distribution of correlated electron pairs, ejected from W(0 0 1), Fe(1 1 0) and Cu(0 0 1) following the impact of a low-energy electron, show characteristic structure that can be associated with the diffraction of two-electron quasi-particles from the periodic surface potential. In this combined theoretical and experimental work we show that the positions of these features in momentum space are determined by the amount of change of the center-of-mass wave vector of the pairs with respect to the surface reciprocal lattice vector. This corresponds to a two-particle Bragg diffraction. The relative intensities of the peaks and the shapes of the peaks depend mainly on the internal correlation of the electron pair, i.e. on the strength of the electronic interaction.

Keywords: Electron emission; Low energy electron diffraction (LEED)

1. Introduction

Low-energy electron diffraction (LEED) is a phenomenon that occurs when a low-energy electron is elastically scattered from a periodic crystal potential. The diffraction is a result of the wave nature of the electron combined with the periodicity of the scattering potential. The latter implies that the potential can absorb only discrete amounts of momentum determined by a reciprocal lattice vector. In case the wave vector of the incoming electron and the crystal structure are known, the positions of the diffracted beams can be determined from the Bragg condition. This simple picture of diffraction has to be modified when a composite particle with internal degrees of freedom (and an appropriate wavelength) is scattered from a crystal surface. In this case the change in the internal motion upon the collision has to be accounted for. The simplest example of this situation is the propagation of an excited, correlated electron pair through a periodic crystal potential out to the vacuum where both electrons can be detected. The internal electron–electron scattering (mediated by the electron–electron interaction) implies that only the total wave vector of the pair is a good quantum number whereas the individual electron's wave vectors are not. When the electron pair is scattered from a periodic potential, the total wave vector of the pair may change by a multiple of the reciprocal lattice vector of the periodic structure. Therefore it is more appropriate to consider the diffraction of the electron pair rather than the diffraction of the individual electrons. It

* Corresponding author. Tel.: +49-345-5582619; fax: +49-345-5511223.

E-mail address: samar@mpihalle.de (S. Samarin).

0039-6028/00/$ - see front matter
PII: S0039-6028(00)00850-5

should be emphasized here, that this observation is independent of the specific scattering mechanism of the electron pair from the crystal. It relies only on the fact that the electrons may change their wave vectors during the collision for reasons other than the elastic scattering from the crystal (here, due to the internal electron–electron correlation) while the total wave vector of the pair is invariant up to a multiple of the reciprocal lattice vector. In fact it can be shown that when the electron–electron interaction is neglected the pair diffraction reduces simply to a diffraction of each of the individual electrons, independently. Thus, it can truly be argued that an observation of the electron pair diffraction is a manifestation of electronic correlation. In this paper we show how the electronic correlation reveals itself in the diffraction pattern of the electron pair and discuss which information can be accessed by studying the diffraction beams.

The excited electron pair can be generated by an electron or a photon impact [1–3]. In the low-energy electron-pair generation by an impinging electron beam, the so-called (e,2e) experiment, the incident electrons have an energy in the range of 20–100 eV. The two excited electrons escape from the sample and are detected in coincidence in the same hemisphere that contains the incident beam (this scattering geometry is called the back-reflection mode). Our coincidence electronics and low primary intensity insure that only those electron pairs are collected that are emitted simultaneously after the impact of one single electron. When the electron pair emerges into the vacuum the (asymptotic) energies and emission angles of the electrons can be resolved. This work provides experimental and theoretical evidence for electron pair diffraction from surfaces. It is concluded that the relative intensities of the diffraction maxima as well as their shapes are largely determined by the internal degree of freedom of the electron pair, i.e., by the interelectronic correlation.

2. Theoretical description

We consider the situation where a low-energy electron beam incident with momentum $\boldsymbol{k}_0$ generates an excited electron pair. The two correlated electrons propagate out to the vacuum and arrive at the detectors with wave vectors $\boldsymbol{k}_1$ and $\boldsymbol{k}_2$.

The Hamiltonian describing the incoming electron beam and the solid surface can be written in the form $H = H_s + H_{ee} + H_{es}$. For simplicity we omit from our discussion the plasmon and the phonon fields, i.e., the frequencies of the incoming and outgoing electrons are off-resonance with the plasmon frequencies of the metallic surface and we neglect inelastic processes. The Hamiltonian of the undisturbed surface is H_s and it describes the electrons in the surface static potential whereas H_{ee} is the interaction within the excited electron pair. The interaction of the incoming electron with the crystal surface is indicated by H_{es}.

The spin-dependent transition operator can be derived to (within certain approximations specified in Ref. [4]): $T^S = (1 + (-1)^S P_{12})T$, where S is the total spin of the electron pair (with $S = 1$ ($S = 0$) corresponding to the triplet (singlet) channel) and P_{12} is a permutation operator that exchanges the two excited electrons. The T operator has the form $T = H_{es}G_0^- + H_{ee}(1 + G_{ee}^- H_{es})$ where G_{ee}^- and G_0^- are the electron–electron and the free propagators, respectively. Thus, for the numerical evaluation of the transition amplitudes the matrix elements $\langle \boldsymbol{k}_1, \boldsymbol{k}_2 | T | \boldsymbol{k}_0, \chi_{\varepsilon(\boldsymbol{q})} \rangle$ are needed. Here $|\chi_{\varepsilon(\boldsymbol{q})}\rangle$ is a single particle eigenstate of H_s with energy ε and crystal momentum $\boldsymbol{q}$, i.e. a bound electron in the valence band.

As we are considering pair-dependent quantities, such as diffraction of the pair, it is more appropriate to transform to a space spanned by $\boldsymbol{K}^+ \otimes \boldsymbol{K}^-$ where $\boldsymbol{K}^+ = \boldsymbol{k}_1 + \boldsymbol{k}_2$ is the center-of-mass wave vector of the pair. $\boldsymbol{K}^- = \frac{1}{2}(\boldsymbol{k}_1 - \boldsymbol{k}_2)$ is the interelectronic relative wave vector that describes the internal degree of freedom of the pair (this is only valid under the assumption that the electronic interaction is mainly dictated by the interelectronic distance).

The periodicity of the scattering potential in the layers parallel to the crystal surface implies Bloch's theorem for the two-particle state. This in turn leads to the conclusion that regardless of the actual functional form of H_{es}, the transition amplitudes $\langle \boldsymbol{k}_1, \boldsymbol{k}_2 | T | \boldsymbol{k}_0, \chi_{\varepsilon(\boldsymbol{q})} \rangle$ can be expressed as [5,6]:

$$\langle \boldsymbol{k}_1, \boldsymbol{k}_2 | T | \boldsymbol{k}_0, \chi_{\varepsilon(\boldsymbol{q})} \rangle = c \sum_{l, \boldsymbol{g}_\parallel} \delta^{(2)}(\boldsymbol{k}_{0\parallel} + \boldsymbol{q}_\parallel + \boldsymbol{g}_\parallel - \boldsymbol{K}_\parallel^+) \times L(\boldsymbol{g}_\parallel, l, \boldsymbol{K}^+, \boldsymbol{K}^-, \boldsymbol{q}) + \delta^{(2)}(\boldsymbol{k}_{0\parallel} + \boldsymbol{q}_\parallel - \boldsymbol{K}_\parallel^+) L'. \quad (1)$$

Here $\boldsymbol{g}_\parallel$ is a surface reciprocal lattice vector. The functions c, L, L' depend on the description of the momentum-space wave function $\chi_{\varepsilon(\boldsymbol{q})}(\boldsymbol{p})$ of the bound electron and on the functional form used for the crystal surface potential H_{es}. For the following numerical calculations we employ a muffin-tin potential for H_{es} as described in Refs. [5,6] and expand G_{ee} to first order in the electron–electron interaction H_{ee}. For the latter coupling we use a screened Coulomb potential with the screening constant being estimated from the Thomas–Fermi model.

Regardless of these limitations for the calculations of L and L' in Eq. (1), some important conclusions can be drawn from the functional form of Eq. (1):

(1) Only the center-of-mass wave vector $\boldsymbol{K}_\parallel^+$ of the pair enters in the Bragg diffraction condition, expressed by the delta function in Eq. (1). This is equivalent to the diffraction of a quasi-particle located at the pair's center of mass when $\boldsymbol{K}_\parallel^+$, the parallel component of its wave vector, is changed by $\boldsymbol{g}_\parallel$ during the collision. We note that in LEED studies diffraction occurs when the change in the wave vector $\boldsymbol{k}_{0\parallel}$ of the incident electron matches $\boldsymbol{g}_\parallel$ [7,8]. The decisive difference to the pair's diffraction is that a fixed $\boldsymbol{K}^+$ does not imply fixed $\boldsymbol{k}_1$ and $\boldsymbol{k}_2$ since a momentum exchange between the two electrons (the internal coordinate $\boldsymbol{K}^-$ changes then) does not necessarily modify $\boldsymbol{K}^+$. This may occur, for example, if the two electrons change their individual wave vectors because of mutual repulsion, while their common center of gravity maintains the value of $\boldsymbol{K}^+$.

(2) While $\boldsymbol{K}_\parallel^+$ determines the positions of the diffraction peaks, the functional dependence of L and L' on $\boldsymbol{K}^-$, which characterizes the strength of the electronic correlation (in our approximation, W_{ee} depends only on $|\boldsymbol{K}^-|$ in reciprocal space), controls the intensity of the individual diffraction peaks. Furthermore, the shape of the individual peaks is influenced by the interelectronic correlation because the cross-section of the (e,2e) reaction depends strongly on the amount of screening in the Coulomb interaction.

(3) The wave vector $\boldsymbol{q}_\parallel$ of the initially bound Bloch electron is not fixed in the experiment and may vary from 0 to $\boldsymbol{k}_{\mathrm{F}}$ (Fermi wave vector). This results in a broadening of the diffraction pattern even in the case where $\boldsymbol{K}^+$ and $\boldsymbol{k}_0$ are experimentally sharply resolved.

(4) Conversely, in case where $\boldsymbol{K}_\parallel^+$, $\boldsymbol{g}_\parallel$ and $\boldsymbol{k}_{0\parallel}$ are well defined, the position and widths of the diffraction peaks reflect the character of $\boldsymbol{q}_\parallel$. For example the maximum width of the diffraction peak is defined by $\boldsymbol{k}_{\mathrm{F}}$. $\boldsymbol{K}_\perp^+$, $\boldsymbol{g}_\perp$, $\boldsymbol{k}_{0\perp}$ are still not defined.

In the arrangement of Fig. 1 the energy conservation law implies a limit for the variation of the wave vector $\boldsymbol{K}_\parallel^+$, i.e.

$$-\sin\alpha_1 \sqrt{2E_{\mathrm{tot}}} \leqslant |\boldsymbol{K}_\parallel^+| \leqslant \sin\alpha_2 \sqrt{2E_{\mathrm{tot}}}, \quad (2)$$

where $E_{\mathrm{tot}} = E_1 + E_2$ is the sum energy of the two electrons, the angles α_1 and α_2 determine the positions of the detectors with respect to the surface normal and are shown in Fig. 1.

The cut-off condition (2) restricts the width of the diffraction peaks, in particular when a

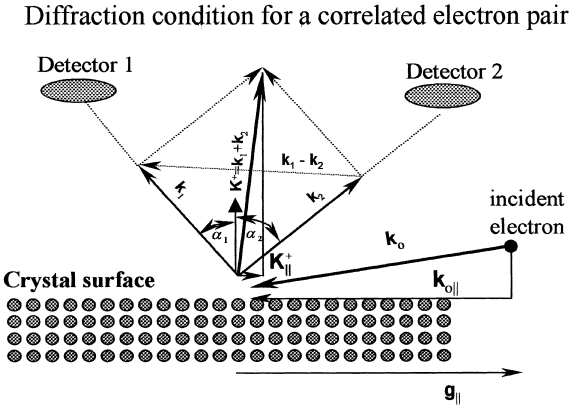

Fig. 1. The geometrical arrangement of the experiment for grazing incidence – illustration of the diffraction condition for an electron pair. $\boldsymbol{K}^+$ is the total momentum of the pair, $\boldsymbol{k}_1$ and $\boldsymbol{k}_2$ are the momenta of the individual electrons, $\boldsymbol{g}_\parallel$ is the surface reciprocal lattice vector, $\boldsymbol{k}_0$ is the momentum of the incident electron with its component $\boldsymbol{k}_{0\parallel}$ parallel to the surface. Without the participation of $\boldsymbol{g}_\parallel$ everything would be strongly peaked in the forward direction and no diffracted pair would be detected.

diffraction beam occurs at the edges of the wave-vector interval given by Eq. (2).

3. Experiment

The (e,2e) experiment in back-reflection geometry using low-energy primary electrons has been designed to achieve surface sensitivity and to study the scattering of correlated pairs from a single crystal surface. The experimental setup is described elsewhere [9]. Here only a brief description of the experiment is given. Two position-sensitive microchannel-plate detectors are used to detect pairs of electrons emerging from a sample surface upon the excitation by a pulsed electron beam. The energies of the electrons are measured individually using a time-of-flight technique. To have a reference point on the time scale the incident beam is pulsed (pulse width about 1 ns) with 2 MHz repetition rate. The flight distances L between the sample and the detectors are 160 mm. The energy resolution of the time-of-flight analyzer depends on the energy E to be measured: $\Delta E = 0.118(E^{3/2}/L)\Delta t$, where L is the flight distance in cm, and Δt is the time resolution in ns. In the range of electron energies used here the energy resolution is 0.3 eV (for $E = 10$ eV) to 3.4 eV (for $E = 60$ eV). The acceptance angle of each detector in the scattering plane is $\pm 13°$. The angle between the detectors' centers is 80° (for the measurements on W(0 0 1) and Cu(0 0 1)) and 100° (for the measurements on Fe(1 1 0)). We used normal (and 2° and 5° off-normal) incidence for the measurements on Cu(0 0 1) and Fe(1 1 0) and grazing incidence (incident angle of 2°) for the measurements on W(0 0 1). The geometrical arrangement for the grazing incidence is shown in Fig. 1. The standard cleaning procedure appropriate for each sample was applied before each measurement under a base pressure in the 10^{-11} mbar range. The cleanliness of the surface was monitored using Auger electron spectroscopy and LEED. The surface was assumed to be "clean" if in Auger spectrum peaks of main contamination (O and C) were on the level of the noise and sharp diffraction patterns of the studied surface were observed in the LEED.

4. Results

We present here the set of experimental data in the form of total parallel momentum distributions. Each of these distributions shows the number of detected electron pairs with a certain total energy as a function of their total wave vector $\boldsymbol{K}_{\parallel}^{+} = \boldsymbol{k}_{1\parallel} + \boldsymbol{k}_{2\parallel}$. We call these distributions "(e,2e) spectra" in this context. It is seen from Eq. (1) that the correlated electron pairs can be emitted only when the component $\boldsymbol{K}_{\parallel}^{+}$ of the total wave vector of the pair fulfils a diffraction condition. On the other hand, we can detect these pairs only when the diffraction condition overlaps with the accessible range of $\boldsymbol{K}_{\parallel}^{+}$ (see Eq. (2)). By changing the experimental conditions, e.g. different incident energy or different crystallographic orientation, we can vary the positions of the diffraction beams in the $\boldsymbol{K}_{\parallel}^{+}$ spectra and we can furthermore control the accessible range of $\boldsymbol{K}_{\parallel}^{+}$. The intensities and the shapes of the diffracted beams are determined by the dynamical factors L and L' (see Eq. (1)).

To outline the role of a pair diffraction we measured the (e,2e) spectra under different experimental conditions: different incident electron energies, various angles of incidence and detection, different lattice constants in the scattering plane (same crystal but different orientation). We performed measurements for different crystals: W(0 0 1), Fe(1 1 0), Cu(0 0 1) with different lattice constants and different orientations of the sample surface.

4.1. W(0 0 1), grazing incidence

To uncover the contribution from the electron pair diffraction in the (e,2e) spectra we performed experiments in a grazing-incidence mode where the diffraction condition is fulfilled with $\boldsymbol{K}_{\parallel}^{+}$ being in the experimentally accessible range (cf. Eq. (2)). For this experiment we used a W(0 0 1) surface with an angle of incidence of 2° with respect to the surface. The (0 1) direction of the crystal surface was in the scattering plane. The geometry of the experiment is shown in Fig. 1. For this geometrical arrangement the incident electron energy was varied in the range 16–22 eV. In this situation the diffraction condition for electron pairs is fulfilled

for $\boldsymbol{K}_{\parallel}^{+}$ being near the middle of the accessible range of $\boldsymbol{K}_{\parallel}^{+}$. Varying the primary-electron energy (the wave vector $\boldsymbol{k}_{0\parallel}$ is then varied) we can control the position of the diffraction maximum in the (e,2e) spectrum. Fig. 2 shows the (e,2e) spectra for different primary-electron energies E_0 but for the same valence electron binding energy $E_b = -1 \pm 0.5$ eV relative to the Fermi level. The arrow in each spectrum corresponds to that $\boldsymbol{K}_{\parallel}^{+}$, which fulfils the diffraction condition (1) with $\boldsymbol{g}_{\parallel} = (-1, 0)$ and assuming $\boldsymbol{q}_{\parallel} = 0$ ("clean" diffraction condition). In reality the valence electron which participates in the collision may have $\boldsymbol{q}_{\parallel}$ in the range from 0 to $\pm\boldsymbol{k}_F$. This broadens the diffraction peak by $2\boldsymbol{k}_F$. The solid lines in Fig. 2 show the calculated spectra. It is seen that when the primary-electron energy increases, the position of the maximum in the spectra shifts, following the diffraction conditions. The calculated spectra reproduce this tendency: the maximum in the spectrum moves towards higher $\boldsymbol{K}_{\parallel}^{+}$ when the incident electron energy increases. The theoretical curves describe qualitatively the shape of measured spectra for low primary energies ($E_0 = 16.1$ eV and $E_0 = 17.2$ eV). In the calculated spectra the integration over all possible values of $\boldsymbol{q}_{\parallel}$ were performed. For higher primary energies the discrepancies between calculated and measured spectra become substantial, especially at the wings of the spectra. One of the reasons for this discrepancy might be the discrimination in the detection of very low energy electrons in the experiment. This is because the large $\boldsymbol{K}_{\parallel}^{+}$ means that one of the electrons of the pair has small energy whereas the second one has almost all energy of the pair. The discrimination of the low-energy electron detection is due to the finite coincidence time window that is set by electronics. The width of the time window determines the lowest energy of electrons that can be detected at a certain primary energy and flight distance. For $E_p = 20$ eV, flight distance 16 cm and coincidence time window 160 ns the minimum energy of electrons that can be detected is about 1.5 eV. On the other hand, in the calculation the detectors were considered as point-like ones, as opposed to our experimental acceptance angle of $\pm$ 13°. In addition only the exchange interaction but not the spin–orbit interaction has been incorporated in the theory. For these reasons, one should not expect a complete agreement of experiment and theory. Further details of the theory and its limitations have been discussed in Refs. [5,6].

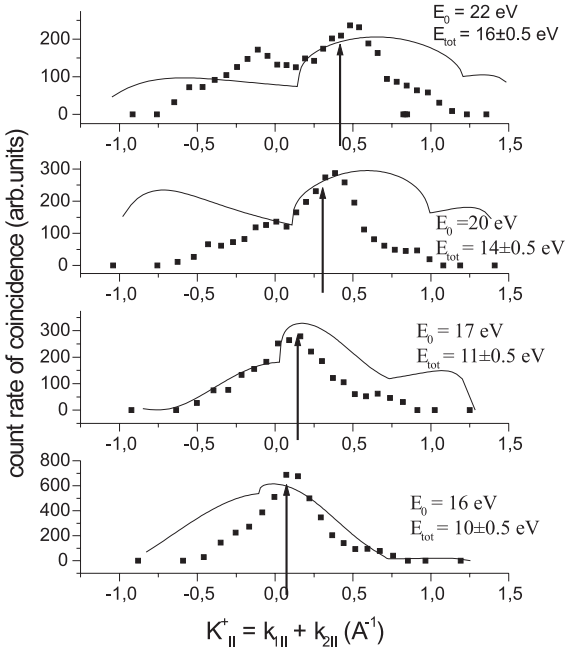

Fig. 2. The (e,2e) distributions of correlated electron pairs excited from W(0 0 1) at 2° angle of incidence with respect to the surface (geometry is shown in Fig. 1). The incident electron energy is E_0 while the total energy of each pair is E_{tot}. Dots are the experimental results, solid curves are the calculated ones. $\boldsymbol{K}_{\parallel}^{+} = 0$ means that the sum momentum vector of each pair points perpendicular to the surface. This does not mean that individual momenta $|\boldsymbol{k}_1|$, $|\boldsymbol{k}_2|$ are equal.

4.2. Fe(1 1 0), near normal incidence

As mentioned above the correlated electron pairs can be detected only when the component of the total wave vector of the pair parallel to the surface belongs to the experimentally accessible range given by Eq. (2). Varying the angles α_1 and α_2 we can change the accessible range of $\boldsymbol{K}_{\parallel}^{+}$ and hence change the contribution of the diffracted pairs to the spectrum. Fig. 3 shows the $\boldsymbol{K}_{\parallel}^{+}$ distributions of the correlated pair excited from Fe(1 1 0), by primary electrons with the energy $E_0 = 50$ eV and with total energy of the pair being $E_{tot} = 44 \pm 1$ eV. The

angle of incidence is 2° with respect to the surface normal. Using the position sensitivity of the detectors we varied the accessible range of $K_{\parallel}^{+}$ by selecting events with larger or smaller angles α_1 and α_2. Vertical solid and dashed lines show the accessible ranges of $K_{\parallel}^{+}$ for two sets of measurements respectively: with large angles ($\alpha_1 = 59°$, $\alpha_2 = 53°$) and small ones ($\alpha_1 = 47°$, $\alpha_2 = 41°$). The larger angles correspond to the larger range of $K_{\parallel}^{+}$ that is accessible for the measurements. The "clean" diffraction conditions (i.e. $q_{\parallel} = 0$) are shown by arrows, which are outside the accessible range of $K_{\parallel}^{+}$. Nevertheless, the broadening of the diffraction peaks due to the finite value of the valence electron wave vector (shaded areas in Fig. 3) allows to observe the contribution of diffracted correlated pairs. Fig. 3 shows that narrowing of the accessible range of $K_{\parallel}^{+}$ (smaller α_1 and α_2) leads to a lower contribution of diffracted pairs.

Fig. 4 shows another (e,2e) spectrum excited from Fe(1 1 0), by primary electrons with the energy $E_0 = 50$ eV and total energy of the pair $E_{tot} = 44 \pm 1$ eV like above. The angle of incidence is 5° with respect to the surface normal, $\alpha_1 = 50°$ and $\alpha_2 = 50°$. The events are integrated over the acceptance angles of the detectors (±13°). Comparison of the calculated $K_{\parallel}^{+}$ distribution (solid curve) with the experimental one shows fairly good agreement. The minimum in the middle of the distribution is mainly due to the fact that the triplet cross-section vanishes for near symmetric geometry and vanishing parallel component of the total momentum of the pair [5,6]. The different contribution from (0,−1) and (0,1) diffraction peaks is due to the off-normal angle of incidence.

Another way to change the contribution of the diffracted correlated pairs is to change the "clean" diffraction condition by changing the lattice con-

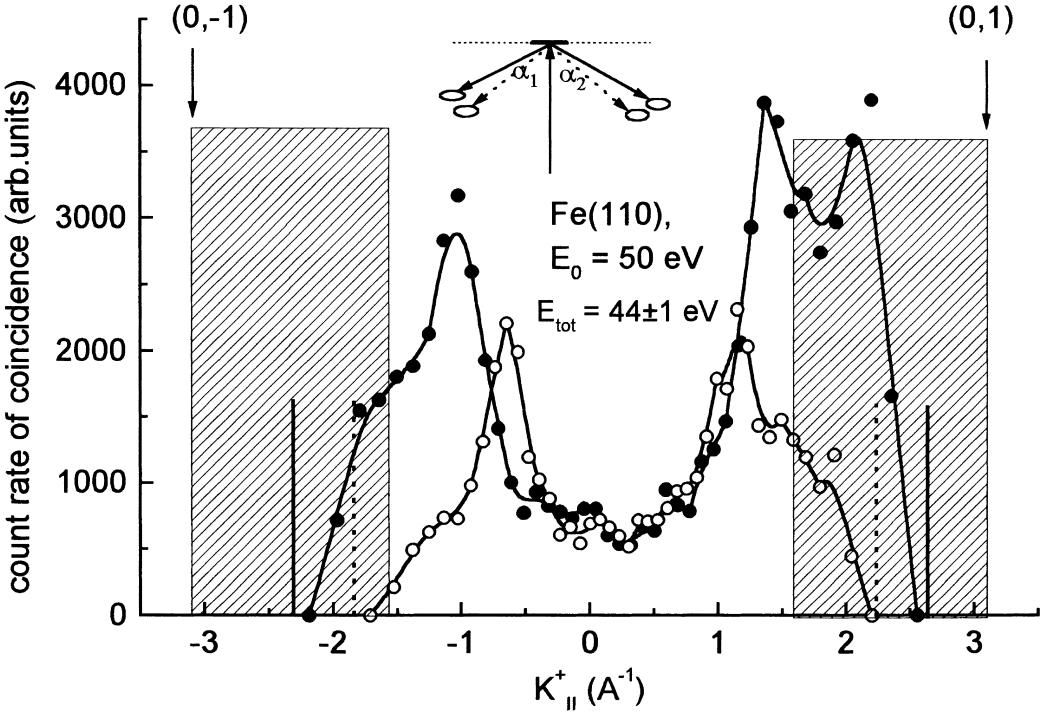

Fig. 3. The total parallel momentum spectrum of correlated electron pairs excited from Fe(1 1 0) by primary electrons with the energy of 50 eV. The total energy of a pair is $E_{tot} = 44 \pm 1$ eV. Solid circles correspond to the larger angles of the detectors $\alpha_1 = 59°$ and $\alpha_2 = 53°$ (shown in the inset). Open circles correspond to the lower angles of detectors $\alpha_1 = 47°$, $\alpha_2 = 41°$. Solid and dashed vertical lines show the limits of $K_{\parallel}^{+}$ corresponding to the two sets of angles. Shaded areas represent the broadening of the diffraction peaks due to the finite value of the valence electron momentum. Vertical arrows denote the "clean" diffraction conditions, i.e. for $q_{\parallel} = 0$.

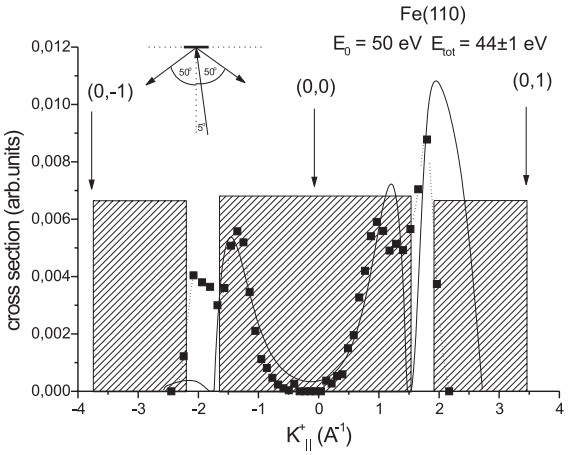

Fig. 4. Comparison of the calculated total parallel momentum spectrum (—) and the experimental one (···) for Fe(1 1 0) excited by primary electrons with 50 eV energy. $E_{tot} = 44 \pm 1$ eV. Shaded areas have the same meaning as in Fig. 3.

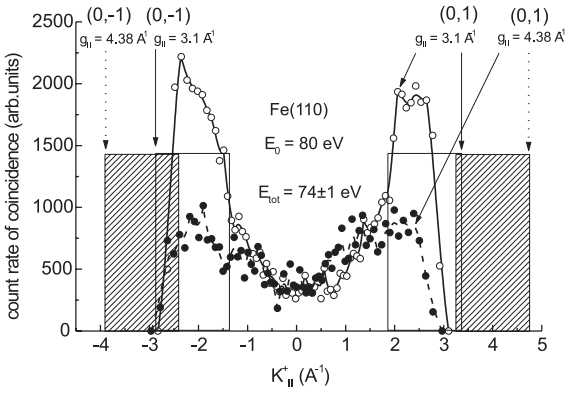

Fig. 5. Total parallel momentum spectra of correlated electron pairs excited from Fe(1 1 0) by primary electrons with 80 eV energy. $E_{tot} = 74 \pm 1$ eV. Solid circles and open circles correspond to two different azimuthal positions of the sample. $\boldsymbol{g}_{\parallel} = 3.1$ Å^{-1} corresponds to scattering within the (0 0 1) plane of the crystal, $\boldsymbol{g}_{\parallel} = 4.38$ Å^{-1} to the (1 $\bar{1}$ 0) plane as the scattering plane. Solid and dotted vertical arrows denote the "clean" diffraction conditions for these two positions of the sample. Shaded and open rectangles show the broadening of diffraction maxima due to the finite value of the valence electron momentum.

stant in the scattering plane and keeping the accessible range of $\boldsymbol{K}_{\parallel}^{+}$ constant. Since we used the two fold symmetric (1 1 0) surface of iron we could change the lattice constant in the scattering plane by rotating the sample about the surface normal by 90°. Fig. 5 shows two spectra for Fe(1 1 0) taken with $E_0 = 80$ eV and $E_{tot} = 74 \pm 1$ eV but for different orientations of the sample. The arrows show the "clean" diffraction conditions for these two cases. In both cases they are beyond the accessible range of $\boldsymbol{K}_{\parallel}^{+}$. But for the position of the sample corresponding to the reciprocal lattice vector in the scattering plane $\boldsymbol{g}_{\parallel} = 3.1$ Å^{-1} the overlap between the broadened diffraction condition (open rectangular area) with the accessible range of $\boldsymbol{K}_{\parallel}^{+}$ (that spans from -3 to 3 Å^{-1}) is larger than for the other sample position ($\boldsymbol{g}_{\parallel} = 4.38$ Å^{-1}). Therefore the contributions from diffracted pairs becomes substantial for the case of the sample position with the reciprocal vector in the scattering plane $\boldsymbol{g}_{\parallel} = 3.1$ Å^{-1}: two maxima in the spectrum at $\boldsymbol{K}_{\parallel}^{+} = -2$ Å^{-1} and $\boldsymbol{K}_{\parallel}^{+} = 2.5$ Å^{-1} rise.

4.3. Cu(0 0 1), normal incidence

The last example shown here is the (e,2e) spectrum for Cu(1 1 0) excited by primary electrons with energy $E_0 = 85$ eV while the total energy of the pairs is $E_{tot} = 79 \pm 1$ eV. Fig. 6 presents the calculated and the experimental spectra. The

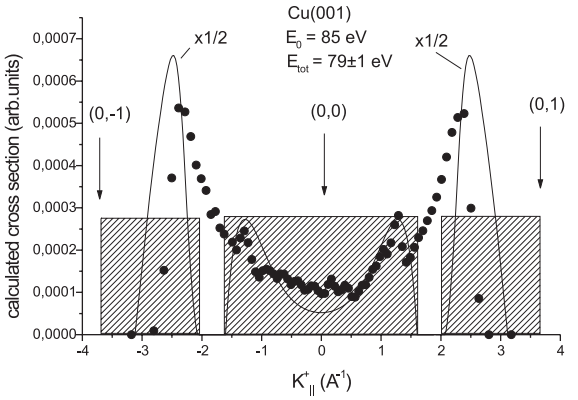

Fig. 6. Momentum-sharing spectrum for Cu(0 0 1) excited by primary electrons with 85 eV energy. $E_{tot} = 79 \pm 1$ eV. Solid line – calculated spectrum, dots – experiment. Diffraction peaks in the calculated spectrum are scaled down by 2. Shaded areas show the range of broadening of diffraction maxima due to the finite value of the valence electron momentum.

theoretical curve (solid line) was calculated for infinite energy- and angle-resolution of the detectors. For clarity the theoretical (0,−1) and (0,1) diffracted peaks are scaled down by 2. The shaded areas show again the broadening of the diffraction peaks due to the variation of the wave vector of the valence electron of the target. The calculated spectrum reproduces fairly well the general shape of the experimental one.

5. Conclusion

As shown above the low-energy (e,2e) spectrum from crystal surfaces is strongly affected by the electron–electron correlation of the emitted pair. This correlation manifests itself, e.g. in the diffraction of the correlated electrons from a crystal surface. In this work we pointed out the conditions under which a diffraction of the pair is possible. Our theoretical arguments have been substantiated by experimental data for a variety of targets.

Acknowledgements

We are grateful to H. Engelhard for his very helpful technical assistance.

References

[1] R. Herrmann, S. Samarin, H. Schwabe, J. Kirschner, Phys. Rev. Lett. 81 (10) (1998) 2148.
[2] S. Samarin, S. Herrmann, H. Schwabe, O. Artamonov, J. Electron. Spectrosc. Relat. Phenom. 96 (1998) 61.
[3] S. Iacobucci, L. Marassi, R. Camilloni, S. Nannarone, G. Stefani, Phys. Rev. B 51 (15) (1995-I) 10252.
[4] J. Berakdar, Probing the spin-polarization in ferromagnets, Phys. Rev. Lett. 83 (24) (1999) 5150–5153.
[5] J. Berakdar, S. Samarin, R. Herrmann, J. Kirschner, Phys. Rev. Lett. 81 (16) (1998) 3535.
[6] J. Berakdar, M.P. Das, Phys. Rev. A 56 (1997) 1403.
[7] J.B. Pendry, Low Energy Electron Diffraction, Academic Press, London, 1974.
[8] M.A. van Hove, W.H. Weinberd, C.-M. Chan, Low Energy Electron Diffraction, Springer Series in Surface Science, Springer, Berlin, 1986.
[9] R. Feder, H. Gollisch, D. Meinert, T. Scheunemann, O.M. Artamonov, S.N. Samarin, J. Kirschner, Phys. Rev. B 58 (1998) 16418.